

Article

Modeling Climatic Influences on Three Parasitoids of Low-Density Spruce Budworm Populations. Part 1: *Tranosema rostrale* (Hymenoptera: Ichneumonidae)

Jacques Régnière ^{1,*} , M. Lukas Seehausen ^{2,†} and Véronique Martel ¹

¹ Natural Resources Canada, Canadian Forest Service Quebec City (QC), QC G1V 4C7, Canada; Veronique.Martel@canada.ca

² Faculty of Forestry, University of Toronto, Toronto, ON M5S, Canada; L.Seehausen@CABI.org

* Correspondence: Jacques.Regniere@canada.ca; Tel.: +1-418-648-5257

† Current address: CABI Switzerland, CH-2800 Delémont, Switzerland.

Received: 29 June 2020; Accepted: 1 August 2020; Published: 5 August 2020



Abstract: Despite their importance as mortality factors of many insects, the detailed biology and ecology of parasitoids often remain unknown. To gain insights into the spatiotemporal biology of insect parasitoids in interaction with their hosts, modeling of temperature-dependent development, reproduction, and survival is a powerful tool. In this first article of a series of three, we modeled the biology of *Tranosema rostrale* at the seasonal level with a three-species individual-based model that took into account the temperature-dependent performance of the parasitoid and two of its hosts. The predicted activity of the first adult parasitoid generation closely matched the seasonal pattern of attack on the spruce budworm, *Choristoneura fumiferana* (Lepidoptera: Tortricidae). The model predicted 1–4 full generations of *T. rostrale* per year in eastern North America. The generations were generally well synchronized with the occurrence of larvae of a probable alternate host, the obliquebanded leafroller *Choristoneura rosaceana* (Lepidoptera: Tortricidae), which could be used as an overwintering host. Spatial differences in predicted performance were caused by complex interactions of life-history traits and synchrony with the overwintering host, which led to a better overall performance in environments at higher elevations or along the coasts. Under a climate warming scenario, regions of higher *T. rostrale* performance were predicted to generally move northward, making especially lower elevations in the southern range less suitable.

Keywords: biodiversity; ecology; environment; forest; global change; insect; parasitoids; spruce budworm; obliquebanded leafroller; seasonal biology; host synchrony

1. Introduction

Parasitoids play an important role as natural mortality factors in population dynamics of insects [1]. However, relatively little is known about the life history and distribution of many. Besides common uncertainties in taxonomy [2], distribution [3], and complex interactions over several trophic levels (e.g., [4]), specific knowledge gaps, such as their seasonal biology, voltinism, and overwintering strategies, restrict detailed understanding. Their frequent dependence on several host species to complete their annual life cycle further impedes the investigation of parasitoid life histories.

Combining empirical data with modeling approaches can help identify and close knowledge gaps that are otherwise difficult to resolve (e.g., [5]). As poikilotherms, insects are strongly dependent on ambient temperature because it determines the rate at which most of their physiological processes occur [6]. Because of its importance relative to other factors, temperature is often used as input in models to better understand and predict changes in insect phenology [6], distribution [7], and overall population dynamics [8].

Few phenology and seasonal biology models have been developed for parasitoids [5,9,10]. Climate warming is expected to have pronounced impacts on parasitoids and their interactions with hosts. They are thought to be particularly vulnerable to increasing temperatures because, in addition to being directly affected, their performance is also determined to a large extent by that of their hosts, which are strongly affected by climate change [11–15]. Different responses to temperature can lead to phenological asynchrony between parasitoids and their hosts, a phenomenon that has been much discussed (e.g., [11,12]). However, the evidence about temperature-induced asynchrony between host-parasitoid relationships and population-level consequences is complex and contradictory [16–18]. Nevertheless, seasonal variation in host availability due to phenological mismatch may impact a parasitoid's spatiotemporal biology and performance [13,19].

The spruce budworm (SBW) *Choristoneura fumiferana* (Clemens) (Lepidoptera: Tortricidae) is a univoltine outbreaking insect with population cycles that last about 35–40 years [20]. Complex interactions of several factors have been found to influence those cycles [21], with parasitoids playing a major role in keeping SBW populations low over long periods [22,23]. We explored the seasonal host interactions in three parasitoids that have a major impact on the population dynamics of their SBW host: *Meteorus trachynotus* (Vier.) (Hymenoptera: Braconidae), which is most important during the decline of outbreaks [21]; *Actia interrupta* (Diptera: Tachinidae), which becomes very common once SBW populations have declined to low density; and *Tranosema rostrale* (Brischke) (Hymenoptera: Ichneumonidae), which succeeds *A. interrupta*, taking over for the remainder of the so-called “endemic” period between outbreaks [24]. *Elachertus cacoeciae* (Hymenoptera: Eulophidae) is another parasitoid that plays an important role as mortality factor at low SBW population densities [22,25]. However, we did not have enough information about this species to model its seasonal biology.

Tranosema rostrale, a koinobiont larval endoparasitoid with a Holarctic distribution, is the subject of this paper. It is viewed as a ‘taxon oligospecialist’ (*sensu* [26]) of tortricid moth larvae in central Europe, and in North America from Alaska to Newfoundland [27]. It has been recorded at very high frequency in low-density SBW populations [24,28], but not everywhere [29], and not at high host densities [4,30]. Spatial variation in parasitism by *T. rostrale* in low-density SBW populations is negatively correlated with warmer climate [22].

The basic biology of *T. rostrale* in North America has been described [24], as well as details about its reproductive biology [31] and its seasonal pattern of parasitism on the SBW [32]. In Quebec, adult females are active in spring when they attack post-diapause SBW larvae and several other Lepidoptera species. Upon egression from the host larva, the parasitoid pupates in a silk cocoon on the foliage next to its host's cadaver, and the adult emerges in late June to early July, after which the parasitoid is suspected of having at least one additional generation. However, it is not clear how soon adults of *T. rostrale* are active in spring, whether there are additional adult generations in summer or autumn, or what alternate hosts the parasitoid exploits following the SBW. The parasitoid is believed to develop in alternate hosts until diapause is induced, but so far, the effort to find its late season hosts in North America has been unsuccessful [24]. *Tranosema rostrale* is not known to parasitize overwintering larvae of SBW [24,29]. Due to its early appearance in spring, it has been hypothesized that *T. rostrale* overwinters as an adult or pupa [24], and in Great Britain, for the same reason, it has been described as overwintering in its cocoon [33]. However, this indirect evidence does not rule out that *T. rostrale* overwinters in a diapausing host larva. Based on the seasonality of the six described alternative host species of *T. rostrale* in North America that also appear across the area of SBW's distribution [24], three are possible late season hosts, that are all tortricids: The wide-striped leafroller *Aphelia alleniana* (Fernald), the large aspen tortrix *Choristoneura conflictana* (Walker), and the obliquebanded leafroller (OBL) *C. rosaceana* (Harris). Only the OBL has been sufficiently studied to be the object of modeling as potential overwintering host of *T. rostrale*. This tortricid overwinters as a third instar larva on the host tree [34]. The frequency of parasitism in wild and implanted OBL larvae by *T. rostrale* is low (<1% and 5%, respectively) among larvae collected in early spring [24]. Parasitism of later OBL generations by *T. rostrale* has not been quantified.

The general goal of this paper is to demonstrate the suitability of individual-based models to study seasonal interactions between trophic levels and climatic influences on multitrophic systems.

We describe the model here in detail because it is applied to other parasitoids of low-density SBW populations. More specifically, we use the model in this paper to (1) gain insights into the temperature-dependent spatiotemporal dynamics of *T. rostrale* in relation to two of its hosts under present and future climates, and (2) raise hypotheses about the parasitoid's unknown seasonal phenology and overwintering biology. To achieve these objectives, we study the impact of synchrony between the parasitoid and two of its tortricid hosts on the performance of *T. rostrale* at the seasonal level. A detailed and well-understood model of SBW seasonal development is available [7]. We develop here an individual-based model for *T. rostrale* based on existing development equations [35]. We also develop a seasonal development model for the multivoltine OBL, based on data from the literature [34,36–38]. In developing this three-species model, we are not interested in the impact of the parasitoid on host populations. Rather, we focus on the impacts of temperature and seasonal variation in host abundance on the performance of the parasitoid (population growth rate) through their effects on oviposition activity (and realized fecundity) and control of the parasitoid's entry into diapause (and overwinter survival). We apply this model to the eastern portion of North America where SBW is often a forest pest problem and investigated the possible impact of climate change on the parasitoid's performance.

2. Materials and Methods

We focused our investigation on the eastern portion of the range of SBW in northeastern North America, from eastern Ontario (80.5°W) to Newfoundland (53°W), and from Pennsylvania (39.7°N) to northern Quebec (52°N) (Figure 1). Seasonality of *T. rostrale* was studied in two sites located in the province of Quebec, Canada: The first near Armagh (46°46' N, 70°39' W, altitude: 270 m), and the second near Petit-lac-à l'Épaulé (hereafter, Epaulé) in the Parc National de la Jacques-Cartier (47°18' N, 71°12' W, altitude: 750 m). The physiography and forest stands in these sites were described by the authors of [39]. Parasitism in those very low-density populations of SBW was monitored biweekly between 1998 and 2019 with implanted host larvae, covering the period of natural larval development in each site using a sentinel technique [32,40]. The technique consisted of placing 100–200 laboratory-reared SBW larvae [41] onto balsam fir foliage in the field, collect them after 7 d, and pursue rearing in the laboratory to determine if they were parasitized. The appropriate larval instar to expose in the field was determined using the SBW seasonal biology model [7]. To determine and describe the pattern of activity of *T. rostrale* beyond the normal period of attack on natural SBW, biweekly implantations of 100–200 fourth instar SBW larvae were pursued in Armagh from the end of June until early August 2016 to monitor attacks by adult *T. rostrale* in the habitat well past the time at which SBW larvae are naturally present. Although *T. rostrale* may not be naturally searching for SBW larvae at that time, it seems to be rather general in its host selection, and this was a simple and effective technique to describe the activity of the parasitoid.

2.1. Modeling the Seasonal Biology of *T. rostrale*

The model of *T. rostrale*'s seasonal biology distinguishes three life stages: The free-living adult, the egg and larval stages inside the host larva, and the pupal stage outside the host (Figure 2a). The parasitoid oviposition module described by [35] was expanded to include a relationship between attack rate and host abundance, which limits oviposition in addition to the balance between oogenesis and egg resorption. The number of attacks by the parasitoid is a function of host density (total number of larvae of both SBW and OBL) and of the number of eggs each female carries in her oviducts. To avoid introducing complex interactions between oviposition history and weather, the maximum attack rate was calibrated to match exactly the maximum oogenesis rate at emergence, with near-empty oviducts, at any given temperature. This was achieved by replacing, in Holling's disk equation [42], the total searching time by the maximum oogenesis rate (O_{\max}):

$$n_a = \frac{a O_{\max} n_h \Delta t}{1 + a t_h n_h}, \quad (1)$$

where n_a is the number of hosts attacked per time interval, n_h is the number of hosts available, a is the search rate, t_h is handling time, and Δt is the size of a time step (0.04167 days, or 1 h). O_{\max} is a function of temperature (after [27]):

$$O_{\max} = \max(0, 0.9555 T - 2.755). \quad (2)$$

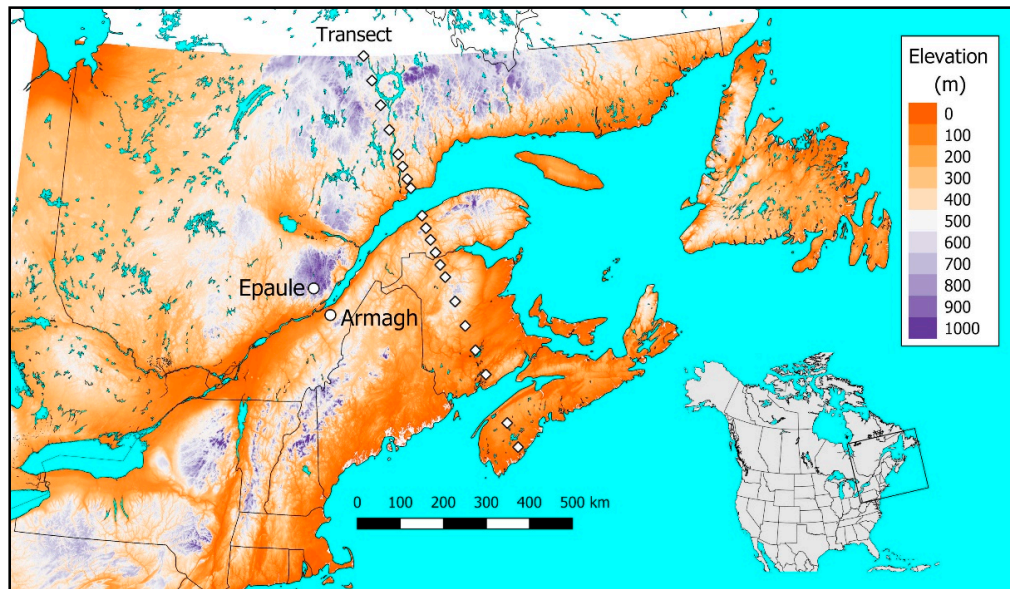


Figure 1. Elevation map of the portion of eastern North America considered in this study. Diamonds: Latitudinal transect locations. Circles: Armagh and Epauleo locations.

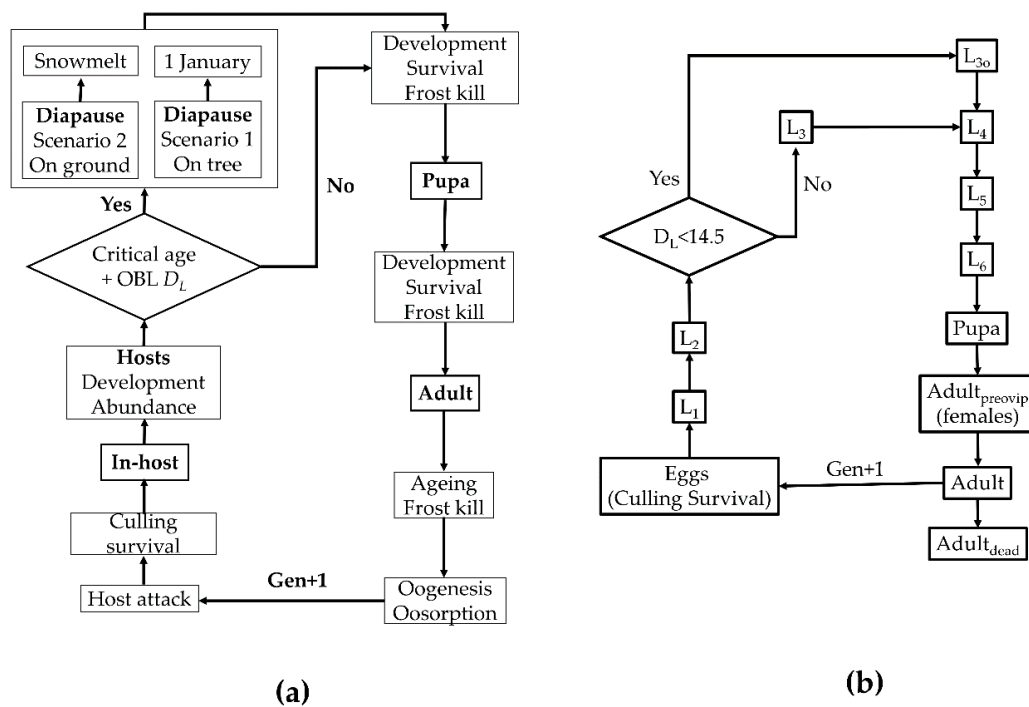


Figure 2. (a) Flowchart of the *Tranosema rostrale* seasonal biology model that distinguishes three life stages (adult, in-host, and pupa). (b) Flowchart of the obliquebanded leafroller (OBL) seasonal biology model. Start 1 January, stop 31 December.

With this formulation, the maximum attack rate is a function of temperature (through its effect on O_{\max}) and host density and ensures that the only influence of search behavior on realized fecundity is directly related to host abundance, not temperature. In other words, the search response is perfectly balanced with the influence of temperature on oogenesis (Figure 3). Parameter values $a = 0.05$ and $t_h = 0.8$ were assigned to scale oviposition activity realistically over the range of host abundance (between 0 and 100 for each host). The specific values were of little importance given the objectives of the model.

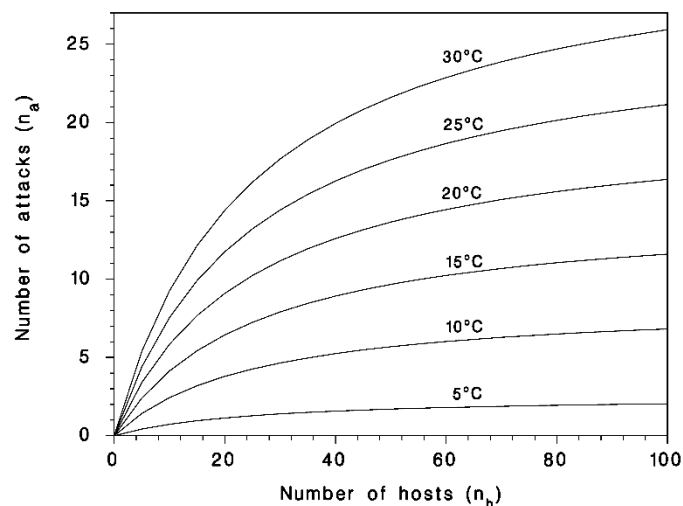


Figure 3. The temperature-dependent functional response of *Traneosema rostrale* (n_a : Number of attacks generated per day per female parasitoid) on larvae of eastern spruce budworm (SBW) or OBL (n_h : Number of hosts). Equations (1) and (2).

Each parasitoid female was assumed to have the entire available host population (feeding larvae of both species) at her disposal. This implies that we also assumed no competition between parasitoids inside the same host. Because the objective was to study synchrony with hosts, not the population dynamics resulting from the parasitoid/host interaction, we think that this simplifying assumption is justified. Finally, before new individuals of the parasitoid were created, culling was applied. The culling survival rate ($0 < S_c < 1$) was a constant that limited the parasitoid's population growth and was adjusted (below) so that the annual growth rate of the parasitoid averaged close to 1. Other mortality of the parasitoid corresponds to the stage-specific, temperature-dependent survival rates [35].

The SBW host emerges from diapause in early spring as a second instar and completes its sixth instar by about late June or early July. Because SBW is univoltine, larvae are available as hosts for a period of about six weeks, starting in May. *Traneosema rostrale* does not attack the first or second instar SBW in late summer, and therefore does not overwinter in this host [30,43]. All SBW individuals in the feeding larval stages (second to sixth), and the parasitoids they contain, are killed by temperatures $< -5^\circ\text{C}$ [7].

We explored two possible diapause scenarios: (1) The parasitized host larva overwinters in the tree as do normal overwintering larvae of the OBL [34], or (2) the parasitoid overwinters either inside a diapausing host larva (such as would occur with *C. conflictana* as overwintering host) or in its cocoon, as hypothesized by others [24,33], in leaf litter under snow cover on the ground. We assumed that entry of the parasitoid into diapause was controlled by the host larva, as occurs often in koinobiont parasitoids [44], although we are not aware of examples from the genus *Traneosema*. Whenever an OBL host is induced into diapause (see below), it also induces diapause in a parasitoid that it contains if the latter has not aged beyond the critical age of diapause onset (a_D). It was also assumed that a diapausing parasitoid had the same cold tolerance as its host [11]. Under Scenario 1, development of the parasitoid resumes in the spring, at air temperature. Under Scenario 2, the parasitoid's development resumes at air temperature only once the snow cover has melted because, prior to that, ambient temperatures are too low for development [5].

2.2. Modeling the Seasonal Biology of the Hosts

SBW development was simulated with the SBW seasonal biology model [7]. The model developed here for OBL phenology is an individual-based, multiple-generation, single-year model that distinguishes 12 life stages: EGG, L₁, L₂, L₃, L₃₀, L₄, L₅, L₆, PUPA, ADULT_{preovip}, ADULT, and ADULT_{dead} (Figure 2b), where L stands for ‘larval stage’ and the subscript numbers for the corresponding instar. Data for the development of a phenology model for the OBL were obtained from [34,36,37]. Stages L₃ and L₃₀ are reached at the same physiological age (3.0), but differ in their development rate function. An individual enters L₃₀ from L₂ in response to exposure to a daylength $D_L < 14.5$ h in either the L₁ or the first half of the L₂. An individual becomes cold-tolerant as soon as it is induced into diapause (L₁ or L₂) and stops developing at molt to the L₃₀. Diapausing L₃₀ larvae can resume development after 1 January as soon as temperatures exceed the lower developmental threshold. If D_L remains > 14.5 h during the L₁ or first half of the L₂, individuals continue development through the L₃ and subsequent stages without entering diapause. All OBL not induced into diapause or in the L₃₀ stage are killed wherever air temperature $T < -5$ °C.

Simulation starts on 1 January and ends on 31 December. The initial population (generation 1) is all L₃₀, 50% male, 50% female. Sexes of OBL differ in their L₆ development (slower in females), with the occurrence of a pre-oviposition period (the ADULT_{preovip} stage) in females and the oviposition process. The oviposition process (females in the ADULT stage) is a simple exponential decay curve, with an initial fecundity of 200 eggs/female. The number of eggs laid per day is given by:

$$E_t = 200\{\exp[-4(A_{t-1} - \text{ADULT})] - \exp[-4(A_t - \text{ADULT})]\} \quad (3)$$

where t is day. To keep numbers of OBL individuals from exploding, a culling rate of 99% (survival: 0.01) is applied to E_t before new individuals are created. Other than freezing, this is the only source of mortality in the OBL population.

All OBL development rates are linear functions of temperature above a lower threshold T_L (parameters in Table 1):

$$r = \begin{cases} a + bT & \text{where } T \geq T_L \\ 0 & \text{otherwise} \end{cases} \quad (4)$$

Table 1. Parameters of the development equation for all life stages of the OBL, *Choristoneura rosaceana*.

Life Stage	a	b	$T_L = -a/b$
EGG [†]	−0.0833	0.008744	9.5
L1 [‡]	−0.14279	0.013027	11
L2	−0.18377	0.018627	9.9
L3	−0.17239	0.0173625	9.9
L3D	−0.11872	0.01069	11.1
L4	−0.08368	0.011875	7.1
L5	−0.12157	0.0138175	8.8
L6 (males)	−0.12648 × 1.23	0.011125 × 1.23	11.4
L6 (females)	−0.12648 × 0.84	0.011125 × 0.84	11.4
PUPA [†]	−0.07901	0.008305	9.6
ADULT_PREOVIP	−0.33918	0.028427	11.9
ADULT [*]	−0.02667	0.0064	4.2

[†] reanalyzed from [37], their Table 1 (same omissions as in original analysis) [‡] all larval stages from [36]. ^{*} No data. Made to allow complete oviposition. Maximum longevity: 30 days.

A correction of L₆ development for the difference between sexes was obtained from [36], where L₆ females took 114 dd and males only 78 dd under the same conditions. Thus, females were 0.84 as fast as the average, and males were 1.23 as fast. These factors were applied to both parameters for the L₆ to ensure a common threshold temperature $T_L = -a/b$ (Table 1). Development stops in all individuals when they enter L₃₀.

2.3. Model Calibration

The data of Aliniaze [38] were used to calibrate the seasonal biology model of the OBL. The only unknown parameter in this model is the variability of development rates. The distribution of individual development rates in all stages was assumed lognormal [45], with a mean of 1 and variance of 0.4. This variance was arrived at by comparing graphically simulated frequencies of immature stages over time to the observations of [38] (Table 1, Figure 4). The OBL model was particularly good at predicting the occurrence of L_3 and L_{30} , using weather data provided by BioSIM [46] for location 44.969°N, −122.933°E, 100 m, at the center of Willamette Valley, Oregon, in 1976. At that location, the model predicted two adult OBL generations, which agrees with the conclusion of [38].

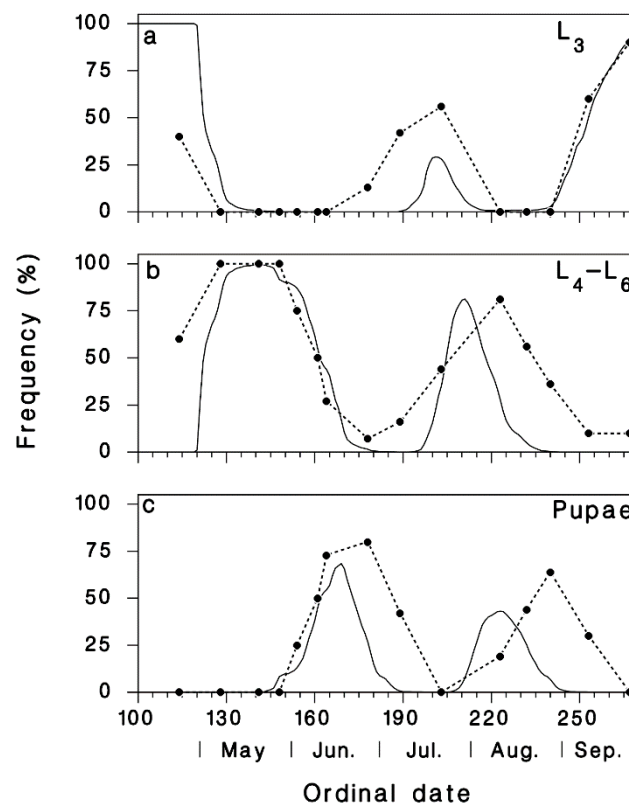


Figure 4. Comparison of observed (●) and simulated (—) frequency of various immature life stages (a–c) of the OBL in the Willamette Valley, Oregon, in 1976 (data from Table 1 in [38]).

To investigate the likelihood of the two overwintering scenarios and calibrate the *T. rostrale* model, a sensitivity analysis to the age of diapause (a_D) was conducted for each diapause Scenario (1 on the tree inside a host, or 2 on the ground inside a host or in its cocoon). The parasitism observations from Armagh and Epauale were divided in two halves: Odd years for calibration and even years for validation. The age of diapause (a_D) was varied systematically: In Scenario 1 between 0 and 0.3 (young larva), and in Scenario 2 between 0.4 and 1.0. Here, $a_D = 1.0$ corresponds to the age of egression and entry into the pupal stage in the cocoon. The optimum value for each scenario was selected based on correlation between observed and simulated attack rates. For this purpose, daily model output was submitted to a seven-day running average (centered) to mimic the seven-day exposure protocol used for field observations. The highest correlation with the calibration of half of the observations was obtained with overwintering Scenario 1, where the parasitoid overwinters as an egg or young larva inside a diapausing host on the tree. The optimum age of diapause was $a_D = 0.15$, or 15% of development inside the host (Figure 5, black symbols). Scenario 2, where the parasitoid overwinters as a more mature larva (optimum at $a_D = 0.7$) inside a host or in its cocoon on the ground under snow cover, yielded slightly lower goodness-of-fit with observations (Figure 5, red symbols). Results of

this sensitivity analysis for overwintering scenarios show clearly that overwintering as a pupa in its cocoon in the soil ($a_D = 1$) was the least likely of all, because the correlation with observations was low (about 0.3). Because Scenario 1 was slightly more plausible, we chose to pursue this work with diapause Scenario 1, using $a_D = 0.15$ as the age of diapause of the parasitoid.

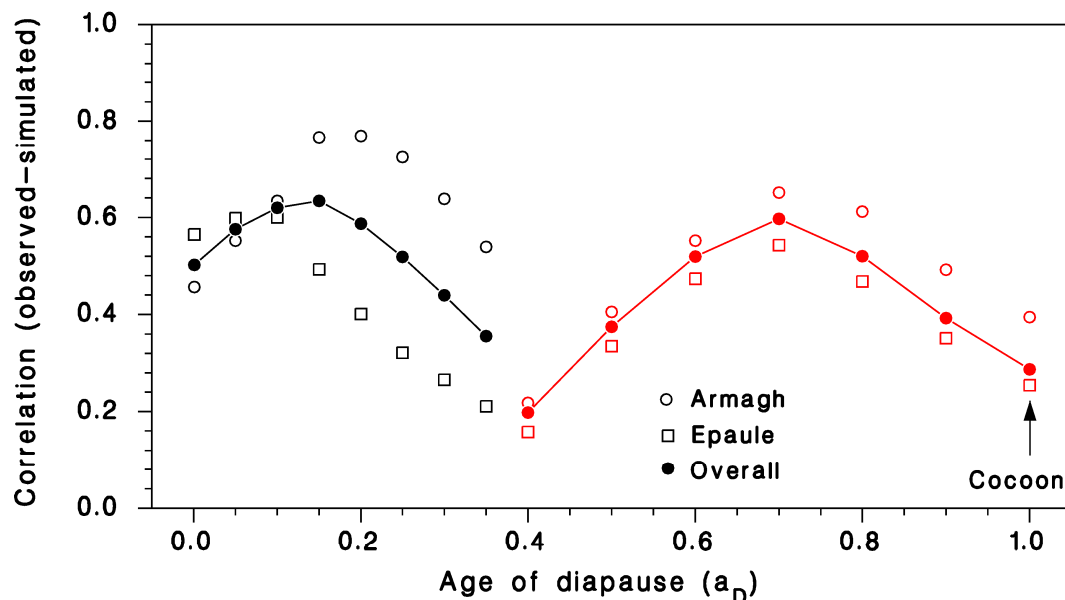


Figure 5. Sensitivity of model output to variation in the age of entry into diapause, expressed as a correlation between observed and simulated oviposition of *Tranosema rostrale* on larvae of SBW. Observations from Armagh and Epaule, in odd years between 1999 and 2017. Black: Diapause Scenario 1 (on the tree); Red: Diapause Scenario 2 (on the ground). Age 0 is newly laid egg, age 1 is pupa in its cocoon. Scenario 1 optimum: $a_D = 0.15$; Scenario 2: $a_D = 0.7$.

The model contains one unknown parameter, the “culling rate” S_c , that determines the absolute value of population growth rate by imposing a low, constant survival rate to all parasitoid progeny. An initial sensitivity analysis of the culling rate was conducted by varying S_c between 0.01 and 0.02 in steps of 0.002, running the model for Armagh and Epaule over the period 1998–2019 using daily minimum and maximum air temperature records as input. The average annual population growth rate R (ratio of total number overwintering in L_{30} hosts in December to the initial 100 individuals) was regressed against S_c . The value $S_c = 0.0147$ produced an average $R = 1$ and was used for all subsequent simulations.

2.4. *Tranosema Rostrale* Performance over Northeastern North America, Present and Future

The three-species simulation model was linked to BioSIM [46] that provided location-specific daily minimum and maximum temperature [47,48] and snow depth inputs [49]. To each simulation point (location), BioSIM matched the four nearest weather stations and applied regional gradients based on the 60 nearest stations to adjust for differences in elevation, latitude, and longitude between weather data source and the simulation point. The daily data from matched stations were averaged using inverse distance as weight. Daily weather records (minimum and maximum air temperature, precipitation) were compiled from all available North American station-based daily air temperature and precipitation measurements. BioSIM can also use monthly normals from which it generates stochastic daily values of minimum and maximum temperatures and precipitation based on the monthly means, variances, and auto- and cross-correlation information that constitute the normals [47,50].

Future climate normals were calculated from daily output of the Canadian Centre for Climate Modelling and Analysis, Canadian Regional Model 4 [51], Canadian Earth System Model 2 [52], and greenhouse gas concentration scenario RCP 4.5 [53]. This particular climate change scenario was

selected because it is a middle-of-the-road (moderate) scenario, with a levelling off of greenhouse gas concentrations near the end of the 21st century that produces a near-center amount of climate change within a 50-year horizon. The forecasted climate model output had 25-km horizontal resolution [54].

The model was run for the Armagh and Epauale locations (circles, Figure 1) in years for which parasitoid attack rate data were available (1998–2019). Because the model is stochastic, each run was replicated 10 times to provide adequate accuracy. We compared observed attack rates, i.e., proportion of sentinel larvae successfully attacked by the parasitoids during successive seven-day exposures in the field, with the predicted frequency of parasitoid adults of the first generation. For this comparison, the maximum predicted frequency of adults was adjusted to match the maximum observed attack frequency on a location and year basis. The seasonality of *T. rostrale* is mostly unknown (but see [24]). To explore its seasonality, we averaged the daily output over years (1998–2019) in both locations.

Maps of potential annual *T. rostrale* population growth rates, defined as the ratio of final number of overwintering parasitoids to the initial number (100), were prepared by running the model for 20,000 randomly located simulation points over northeastern North America between 39°30'N by 81°W and 52°N by 52°30'W. A first map was prepared using as input daily air temperature records over the period 1981–2010. A second map was produced using 30 annual time series of daily minimum and maximum air temperatures generated stochastically from normals for the period 2011–2040, as obtained from the daily output of the climate change model [47,50]. The results were interpolated by universal kriging, using elevation as external drift variable [55] obtained from a Digital Elevation Model at 250-m horizontal resolution (Figure 1).

To help interpret the mapping results, the average temperature over the period 1 May to 30 September (hereafter summer temperature) was calculated for each simulation point. The relationships between summer temperature and average survival, fecundity, and annual population growth rate were graphed for the two periods (observed 1981–2010 and forecast 2011–2040). A series of simulations was also run along a north-south transect of 20 evenly spaced locations (diamonds, Figure 1) between the northern edge of the Manicouagan Reservoir in Quebec (50°N, 69.57°W) and Little Lake NS, just north of Wilkins, Nova Scotia (44°N, 65°W), using daily records for 1981–2010 or 30 years of disaggregated climate change normals for 2011–2040. Model output was averaged by generation (survival rate, fecundity, contribution to the end-of-season overwintering populations) for each location along the transect for each period.

3. Results

3.1. Validation of Predicted Seasonality of *T. rostrale* Attack Rates

Daily oviposition rates output by the model using overwintering Scenario 1, with $a_D = 0.15$ and submitted to a centered seven-day running average, were compared graphically with observed seasonal attack trends on sentinel SBW larvae in Armagh and Epauale in the validation half of the data (even years between 1998 and 2018; Figure 6). The agreement between these independent observations and model output was excellent, especially in Armagh. By contrast, the timing of *T. rostrale* adult activity using Scenario 2 with the parasitoid overwintering on the ground in its cocoon, as suggested by the authors of [33], is much too early compared to observations (shaded curves, Figure 6). In nature, female *T. rostrale* of the second generation would not normally encounter SBW larvae because they would emerge after these larvae have developed to the pupal stage. However, in 2016, when sentinel SBW larvae were implanted in Armagh until early September, well after their natural period of presence, the attack pattern clearly shows the parasitoid's second generation, which corresponds well with the predictions of the model (Figure 6).

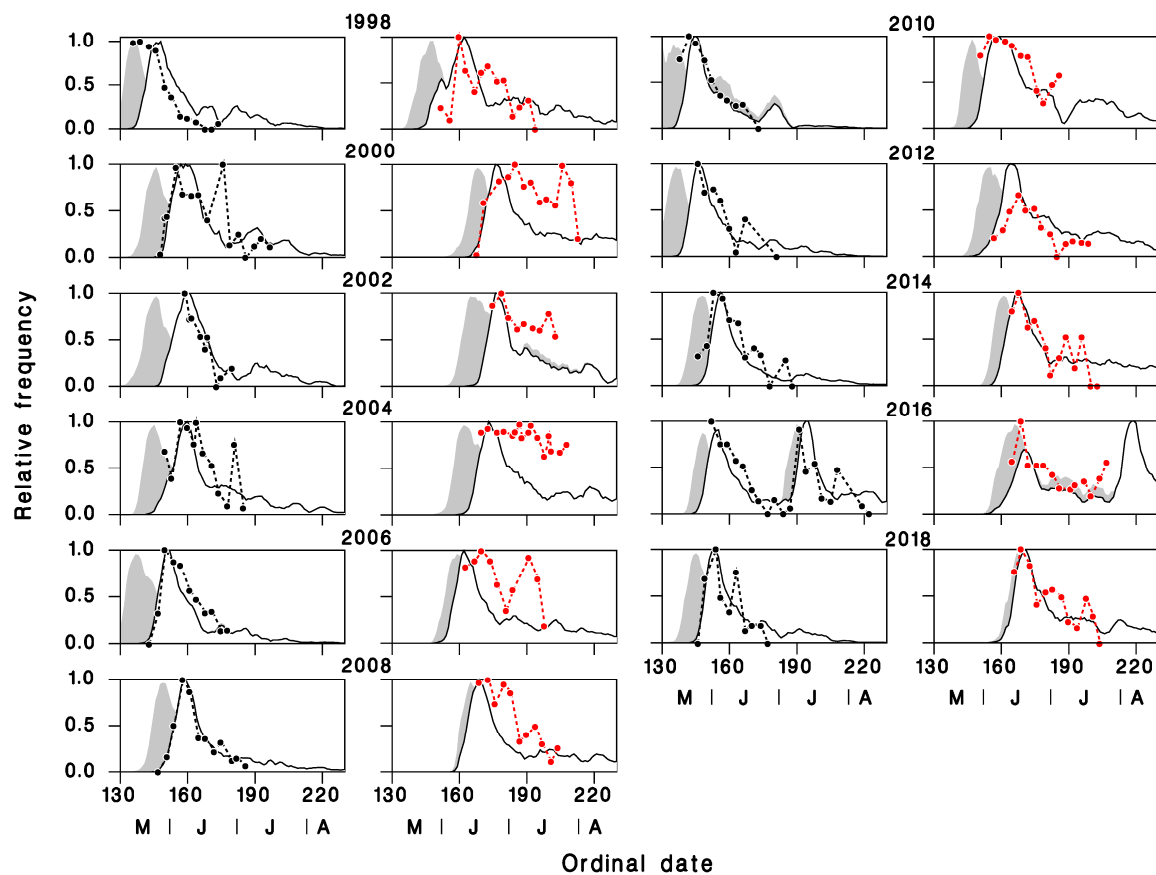


Figure 6. Three-species model output comparison with observations. Solid lines: Diapause Scenario 1 (on tree), age of diapause $a_D = 0.15$. Shaded curves: Scenario 2, overwintering in the cocoon on the ground. Observed (●) seasonal oviposition trends by *Tranosema rostrale*, in even years between 1998 and 2018 (validation subset). Black symbols: Armagh; red symbols: Epaule. In 2016, the line represents oviposition by the first two generations of the parasitoid.

3.2. Seasonal Biology of *T. rostrale*, SBW, and OBL in Armagh and Epaule

In Armagh, the model predicts three complete generations of *T. rostrale* adults, with a partial fourth (Figure 7a). In 2016, we observed the second generation of adults in Armagh using sentinel SBW larvae (Figure 6), but these were stopped in early August, too soon to observe additional generations. In Epaule, only two complete adult generations are expected, with a partial third (Figure 7b). In both locations, first generation adults can attack both SBW and OBL larvae that are feeding simultaneously (Figure 7c,d). In Armagh, the second- and third-generation adults are well timed with feeding OBL larvae (Figure 7c). In Epaule, however, third-generation females of *T. rostrale* encounter few feeding OBL larvae, and because most of those would be nondiapausing, they would be killed by frost later in the fall (Figure 7b,d). The same fate would await the progeny of the parasitoid's fourth adult generation in Armagh (Figure 7a,c).

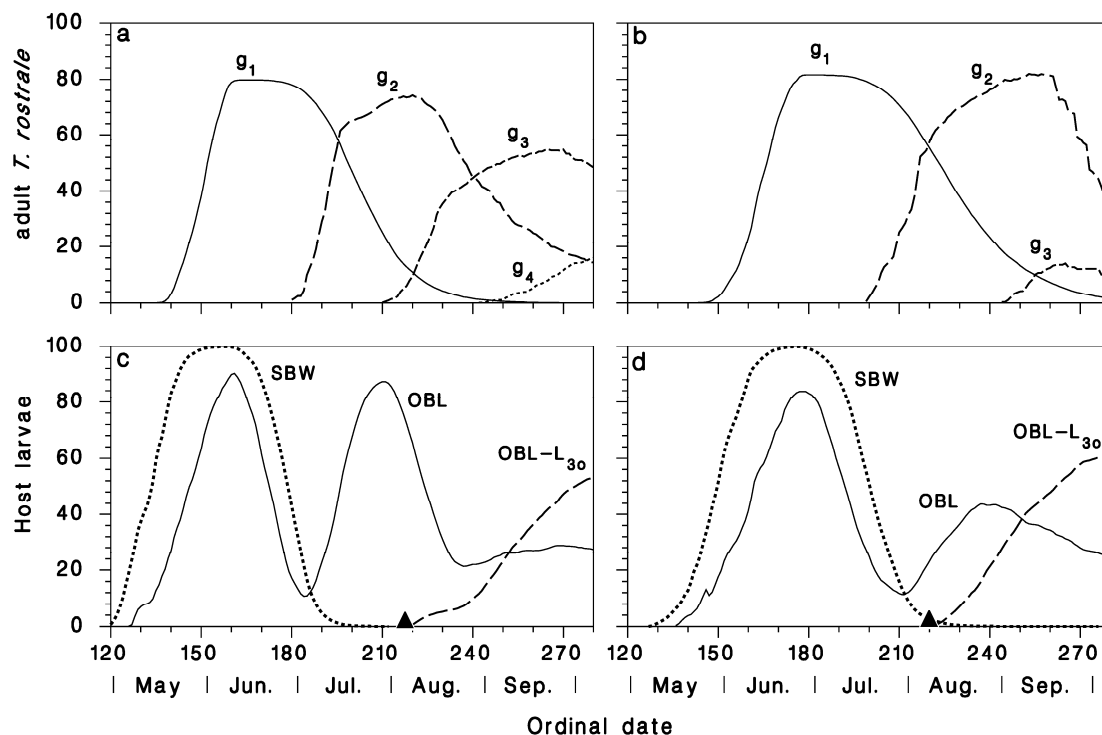


Figure 7. *Tranosema rostrale* model, diapause Scenario 1 (in tree), age of in-host diapause $a_D = 0.1$, averaged over the period 1988–2017 in Armagh and Epaule. Abundance of successive generations of *T. rostrale* adults (initial g_1 to g_4) in (a) Armagh and (b) Epaule. Corresponding abundance of host larvae (SBW:) and OBL (feeding larvae: —, OBL- L_{30} diapausing larvae: - - -) in (c) Armagh and (d) Epaule. ▲: Date when daylength < 14.5 h.

3.3. *Tranosema Rostrale* Performance over Northeastern North America, Present and Future

The spatial patterns of predicted *T. rostrale* population growth rates are complex. Under climatic conditions of the recent past (1981–2010), *T. rostrale* may have had more success as a natural enemy of SBW in cool environments at higher elevations or along the coasts (Figure 8a). Under a middle-of-the-road climate change scenario in the near future (2011–2040 normals from the RPC 4.5 greenhouse gas emission scenario), the parasitoid's distribution can be expected to change significantly, shifting generally northward and becoming less effective at lower elevations in the southern portion of its range (Figure 8b).

Much of the complexity of this spatial pattern resulted from the interactions between summer temperature (May–September), survival (Figure 9a), and reproductive success of the parasitoid (Figure 9b). The combination of these two outcomes, conditioned by synchrony with the susceptible life stages of the OBL, the parasitoid's overwintering host in our model, led to the multimodal pattern of annual population growth rates (Figure 9c). This pattern itself was essentially unaffected by climate change.

3.4. Performance of *T. rostrale* Along a North-South Transect

There was considerable and complex variation of the predicted annual population growth rate of the parasitoid along the north-south transect that resulted from interactions of survival from egg to adult, realized fecundity, and voltinism at each location (Figure 10). Over the period 1981–2010, the growth rate was lowest in the middle of the transect (solid line in Figure 10c) at latitudes between 47° and 49°N, corresponding to locations in northern New Brunswick and the Lower St. Lawrence in Quebec. This drop in growth rate was due to the interaction of voltinism and timing with the overwintering stage of the OBL host. The number of generations of the parasitoid decreased gradually northward, with most overwintering individuals belonging to generations 3, 4, and 5 (Figure 10d). Here, overwintering larvae of generation 5 are the progeny of the 4th generation of adults. Whereas

the same is true over the period 2011–2040 (Figure 10h), growth rates in the future were expected to decrease at the southern and northern edges of the transect, and to increase considerably in the central section in the vicinity of the St. Lawrence River valley (Figure 10g).

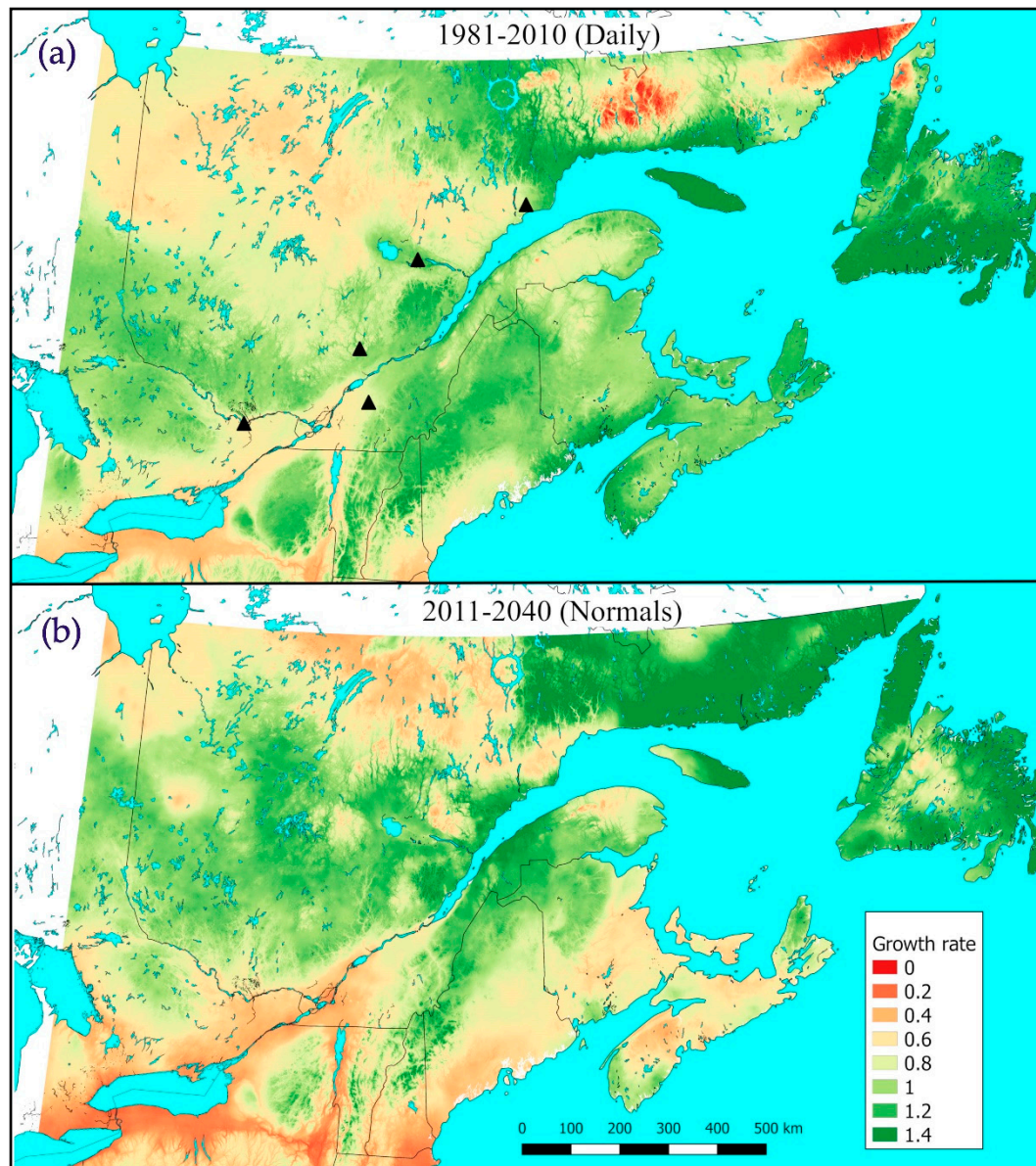


Figure 8. Maps of annual population growth rate of *Tranosema rostrale* over northeastern North America. (a) From 1981–2010 daily minimum and maximum air temperature records. (b) From 2011–2040 normals disaggregated to stochastic daily minimum and maximum air temperature, from the Intergovernmental Panel on Climate Change (IPCC)’s greenhouse gas emission scenario RCP 4.5 [53,54]. Triangles in (a) are locations of SBW outbreak epicenters.

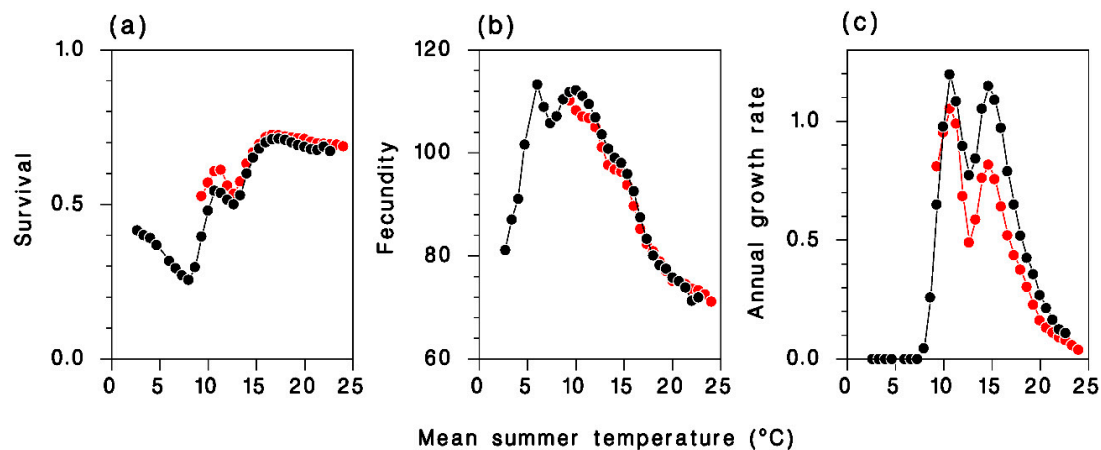


Figure 9. Compilation of average (a) survival of immatures, (b) fecundity of females, and (c) annual population growth rate (measured at the overwintering stage) relative to average summer air temperature (black: From daily air temperature records between 1981 and 2010; red: From climate-changed disaggregated normals 2011–2040).

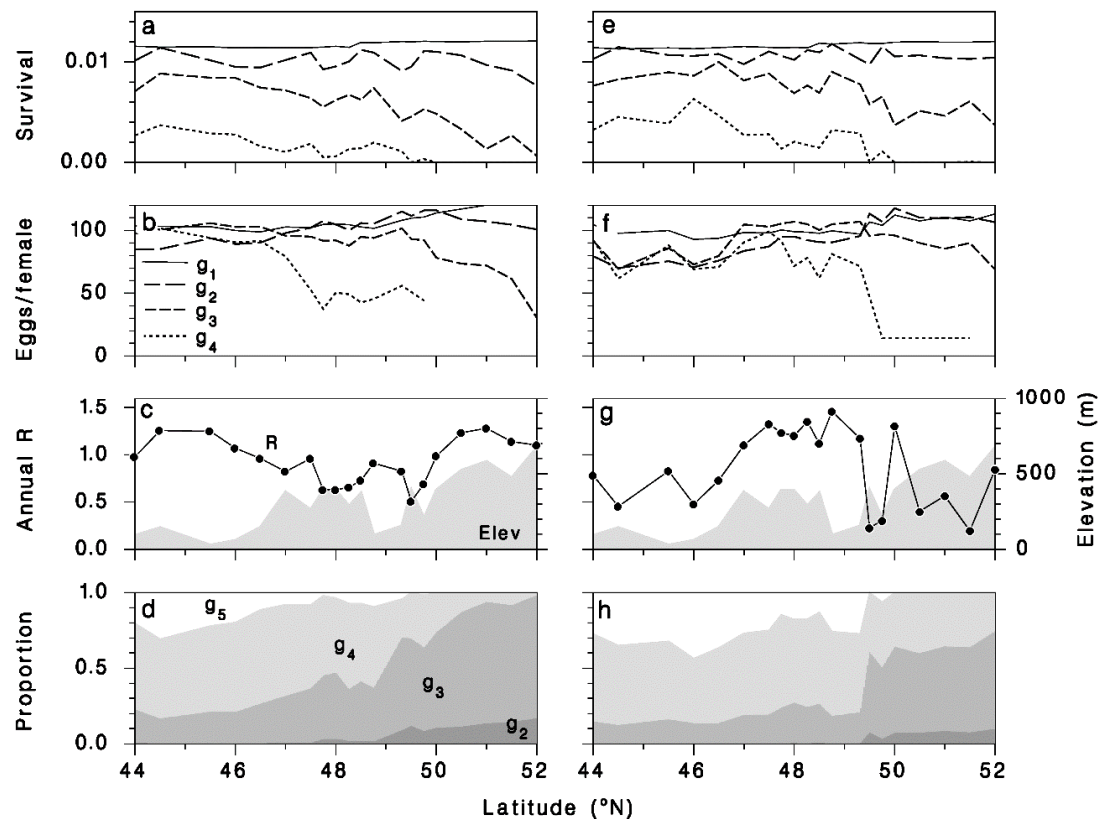


Figure 10. Summary of model output along the north-south transects under (a–d) 1981–2010 climate and (e–h) future climate (2011–2040). (a,e): Survival from egg to adult in each generation (g_1 to g_4 , where g_1 is the initial generation in overwintering hosts in January), including culling survival $S_c = 0.0147$. (b,f): Realized fecundity per female parasitoid. (c,g): Annual population growth rate R , from initial 100 to overwintering in L_{30} of OBL hosts at the end of the year; shaded curve: elevation along the transect. (d,h): Proportion of overwintering parasitoid population contributed by each generation.

4. Discussion

With this individual-based model, we gained insights into the seasonality and spatiotemporal biology of *T. rostrale*. By considering the influence of temperature on its key life history traits,

we simulated its seasonal pattern of attack, voltinism, and potential population growth rate in eastern North America. The model predicted well the observed pattern of seasonal parasitism on SBW larvae in two study areas over a period of 22 years from 1998 to 2019. The fit was particularly good in Armagh (black symbols in Figure 6), and not quite as good in Epaule (red symbols, Figure 6). The Epaule site is characterized by a steep elevation gradient [39], which undoubtedly resulted in increased variability of seasonal development for both hosts and parasitoids, and consequently, the timing of parasitism. Many other factors can influence the seasonal pattern of parasitism, such as competition with other parasitoid species, e.g., the dipteran *Actia interrupta* Curran [56] and the ectoparasitic eulophid wasp *Elachertus cacoeciae* (Howard) [24,25,30]. Abiotic factors other than temperature, such as humidity, rain, and wind, can also affect parasitoid seasonality and activity (e.g., [57]). Weather in Epaule, at 750-m elevation, is more marginal and variable than in Armagh [39].

The model also accurately predicted the timing of the second generation of the parasitoid in summer 2016 in the Armagh study site (Figure 6). Whereas this constitutes validation for the timing of further parasitoid generations, our model was based on parasitoid development rates measured in SBW as a host. These rates may differ slightly in other hosts. The model predicted 1–4 full generations of *T. rostrale* per year within the modeled area (Figure 10d,f). Through rearing in an outdoor insectary, it was determined that this parasitoid can undergo three generations in Quebec City [24]. The model predicted three full generations in Armagh, near Quebec City.

In the European literature, it was stated that this species overwinters in its cocoon [33], based on specimens of *T. rostrale* in museum collections reared from various tortricid hosts. In North America, it was thought to overwinter as a pupa or as an adult [24]. However, given the temperature-dependent development of *T. rostrale* and the observed pattern of seasonal parasitism on SBW larvae, this overwintering strategy is unlikely because the model predicts adult activity of the parasitoid much earlier than observed (shaded curves in Figure 6). This discrepancy between the European literature and our results may be the result of an invalid conclusion about the European parasitoid's overwintering strategy, but it is also possible that *T. rostrale* in Europe and North America are two cryptic species. It also remains possible that *T. rostrale* in North America actually overwinters as a larva on the ground in a larger diapausing host such as the large aspen tortrix. From a first adult generation timing point of view, this scenario is nearly as likely as our Scenario 1 and would not invalidate the conclusions reached with our modeling. These hypotheses warrant further research. In particular, the hypothesis that the OBL is a primary host of *T. rostrale* (i.e., that all parasitoid generations can attack this host and overwinter within it) remains to be confirmed.

Model predictions of the annual parasitoid population growth rate are relative and can only be used to explore the parasitoid's temperature-dependent overall fitness within the modelled habitat, as it interacts with the modeled hosts. However, these relative growth rates provide useful information about the temperature dependence of the parasitoid's performance. In general, *T. rostrale* was predicted to perform better in environments at higher elevations or along the coasts. This spatial distribution of performance reflects the known decreasing survival and fecundity of the parasitoid with increasing temperatures [35], explained as an interaction between SBW's immune system and the parasitoid's polydnavirus [58,59]. Lower rates of SBW parasitism by *T. rostrale* occur in sites where temperatures are higher [22]. However, results of the present study indicate that the complex spatial patterns of parasitoid performance result from interactions of survival from egg to adult, realized fecundity, voltinism, and synchrony with the overwintering host.

Spatial and temporal differences in SBW parasitism by *T. rostrale* have been described for several sites in northeastern North America and have generally been linked to SBW population densities. The impact of *T. rostrale* decreases as SBW populations increase [4,23] and seems negatively affected by the abundance of competing parasitoid species [22,32,56]. In the present model, we used a simple description of density dependence in parasitoid attack, and there was no consideration of either intra- or interspecific competition. Our model suggests that considerable spatial variation in the parasitoid's performance occurs because of temperature-dependent synchrony with hosts. It is interesting that

several locations where the model predicts relatively low parasitoid population growth rates are known epicenter locations of the current SBW outbreak [60] (triangles in Figure 8a). These epicenters have been linked to highly favorable climate, especially through heavy host plant flowering [61] or to moth immigration [62]. However, a generally weak performance of natural enemies in low-density SBW populations may be a contributing factor to the formation of epicenters, although parasitism has been found to be a surprisingly weak predictor of spatiotemporal variation in low-density SBW populations [22]. It is thought that once an SBW outbreak starts, the migration of SBW moths will distribute so many eggs that low-density parasitism will become diluted in sink populations [62].

Under the climate warming scenario applied here, regions of higher *T. rostrale* performance are predicted to generally move northward, making lower elevations in the southern range especially less suitable, and the cooler northern regions generally more suitable. The sensitivity of the parasitoid to high temperatures explains this predicted upward and northward shift. Several modeling approaches applied to data on temperature-dependent performance of the SBW have also predicted a shift in its range toward the north as the climate changes [7,63–65]. It is likely that the OBL's distribution will also shift northward, although this hypothesis has yet to be explored. Thus, if the distribution of both the parasitoid and the host shift northward, no spatial mismatch will occur over most of their distribution. However, warmer regions seem to be less favorable for control of low density SBW populations by parasitoids [22], and given that this study suggests that a spatial mismatch between parasitoid and host may develop under climate change, this increases the likelihood of an outbreak where SBW is still prevalent but the parasitoid's performance is weakened. Some authors have also suggested that a 'temporal refuge' for SBW might develop under a scenario of climate warming due to the differential optima for development of the SBW versus its parasitoids. Such phenological mismatches have the potential to lower overall parasitism of low-density SBW populations, allowing SBW populations to escape control and develop outbreaks [66]. Indeed, the optimum temperature for development of SBW [67] exceeds the optimum for *T. rostrale* [35]. Thus, it is conceivable that SBW may survive better under climate warming because of decreased attacks by natural enemies [68]. However, evidence for temperature-driven mismatches between parasitoids and their hosts is scarce [16,69], and it has been demonstrated that even if present, mismatches in the phenology of interacting species may not have consequences at population levels [18]. Additional complexity is added to our host-parasitoid system because *T. rostrale* is generalist to a certain extent [24,33] and may therefore not necessarily be affected by changes in the distribution of the two hosts modelled here.

5. Conclusions

Understanding the complex impacts of climate change on the ecological interactions between insect parasitoids and their hosts is clearly important [45]. Predicting the responses of parasitoid/host systems to climate change requires a detailed understanding of responses of the species involved because of the diversity of life history choices displayed by parasitoids [45]. The overwintering strategy of *T. rostrale* is not clearly understood [24,33].

Modeling population-level interactions between trophic levels at the seasonal time scale is very well suited to individual-base modeling approaches, because it can handle multidimensional change scenarios and complex interactions [70]. In this paper, we showed that the timing of its first generation of adults that attack feeding larvae of the SBW [24] is most consistent with the hypothesis that the parasitoid overwinters as an egg or as a very young larva inside a diapausing larval host, a strategy known to be that of the other two parasitoids species that constitute this series: *Actia interrupta* [unpublished data of J.-C.T.] and *Meteorus trachynotus* [71]. The timing of first-generation adult attacks by *T. rostrale* on SBW larvae is too late for the parasitoid to overwinter on the ground inside its cocoon, even under snow. For the same reason, its overwintering as an adult, either on the ground or on trees, is even less likely. In the habitat of SBW, the most likely overwintering host candidate is the OBL that spends winter in diapause at the third instar on its host tree [34], although two other

tortricids are possible overwintering hosts in North America: The large aspen tortrix and perhaps the wide-striped leafroller.

Tranosema rostrale has been shown to be adversely affected by warm climate [22,27] as a result of its temperature-dependent immune response [58], as well as that of the host [59]. We confirmed here that the parasitoid is multivoltine, undergoing between two and four complete generations per year, depending on temperature. Whereas its SBW host is strictly univoltine and is not an overwintering host, the OBL is multivoltine, with two to three generations per year, and enters facultative larval diapause after some feeding at the end of summer. The complex synchrony between adults of the parasitoid and the susceptible larval stages of these two hosts generates intricate spatial patterns of expected parasitoid performance. We showed that these patterns were linked to mean summer temperature, and that climate change should not affect them. Rather, it is the geographical distribution of those temperatures that determines the locations in which *T. rostrale* is likely to exert the most control capability on its host of most importance in forestry, the SBW [72]. As argued by Schmitz and Barton [73], our results confirm that the impact of climate, and climate change, on the ecological interactions between natural enemies and hosts are the complex result of behavioral and physiological processes of both parasitoids and hosts. This impact is, in large part, caused by issues of synchrony between natural enemy reproduction and susceptible host stages [74]. These climate-induced patterns vary with topography and geography [75] and can have a profound effect on the population regulation exerted by natural enemies on the dynamics of host populations [76].

Author Contributions: J.R., M.L.S. and V.M. conceived and designed research, and collected field data. J.R. developed the model and did the analysis. M.L.S., J.R. and V.M. wrote the manuscript. All authors read and approved the manuscript.

Funding: This research was supported by financial and in-kind support through SERG-International by the provincial governments of Ontario, Quebec, Newfoundland, Nova Scotia and Saskatchewan and the Société de protection des forêts contre les insectes et maladies (SOPFIM), as well as by the Atlantic Canada Opportunities Agency and Natural Resources Canada. Funding for MLS was provided by the Ontario Trillium Scholarship.

Acknowledgments: Thanks to R. St-Amant for help with model coding and linkage with BioSIM. Thanks to the Insect Production and Quarantine Laboratories of the Canadian Forest Service (Sault Ste. Marie, ON) for providing the SBW larvae used in this study. We also thank P. Duval, S. Trudeau, P. Huron, M. Moisan, and S. Hache for help in the field and laboratory and the Ministère des Forêts de la Faune et des Parcs du Québec (MFFPQ) for insect rearing and parasitoid identification. We thank Mark R. Shaw for his detailed answer to our questions concerning the biology of *Tranosema rostrale* in Europe, and two anonymous reviewers who helped us improve the manuscript.

Conflicts of Interest: The authors declare no conflict of interest.

References

1. Hawkins, B.A.; Cornell, H.V.; Hochberg, M.E. Predators, parasitoids, and pathogens as mortality agents in phytophagous insect populations. *Ecology* **1997**, *78*, 2145–2152. [\[CrossRef\]](#)
2. LaSalle, J.; Gauld, I.D. Parasitic Hymenoptera and the biodiversity crisis. *Redia* **1991**, *74*, 315–334.
3. Quicke, D.L.J. We know too little about parasitoid wasp distributions to draw any conclusions about latitudinal trends in species richness, body size and biology. *PLoS ONE* **2012**, *7*, e32101. [\[CrossRef\]](#) [\[PubMed\]](#)
4. Eveleigh, E.S.; McCann, K.S.; McCarthy, P.C.; Pollock, S.J.; Lucarotti, C.J.; Morin, B.; McDougall, G.A.; Strongman, D.B.; Huber, J.T.; Umbanhowar, J.; et al. Fluctuations in density of an outbreak species drive diversity cascades in food webs. *Proc. Natl. Acad. Sci. USA* **2007**, *104*, 16976–16981. [\[CrossRef\]](#) [\[PubMed\]](#)
5. Régnière, J.; Griffiths, K.J. La modélisation en lutte biologique: Un exemple d'utilisation dans l'étude du synchronisme des cycles vitaux d'un parasitoïde et de son hôte. In *La Lutte Biologique*; Vincent, C., Coderre, D., Eds.; Gaëtan Morin: Boucherville, QC, Canada, 1992; pp. 265–284.
6. Chuine, I.; Régnière, J. Process-based models of phenology for plants and animals. *Ann. Rev. Ecol. Evol. Syst.* **2017**, *48*, 159–182. [\[CrossRef\]](#)
7. Régnière, J.; St-Amant, R.; Duval, P. Predicting insect distributions under climate change from physiological responses: Spruce budworm as an example. *Biol. Invasions* **2012**, *14*, 1571–1586. [\[CrossRef\]](#)
8. Flinn, P.W.; Hagstrum, D.W.; Muir, W.E.; Sudayappa, K. Spatial model for simulating changes in temperature and insect population dynamics in stored grain. *Environ. Entomol.* **1992**, *21*, 1351–1356. [\[CrossRef\]](#)

9. Drummond, F.A.; Van Driesche, R.G.; Logan, P.A. Model for the temperature-dependent emergence of overwintering *Phyllorhynchus crataegella* (Clemens) (Lepidoptera: Gracillariidae), and its parasitoid, *Sympiesis marylandensis* Girault (Hymenoptera: Eulophidae). *Environ. Entomol.* **1985**, *14*, 305–311. [\[CrossRef\]](#)
10. de Souza, A.A.; Martins, S.G.F.; Zacarias, M.S. Computer simulation applied to the biological control of the insect *Aphis gossypii* for the parasitoid *Lysiphlebus testaceipes*. *Ecol. Model.* **2009**, *220*, 756–763. [\[CrossRef\]](#)
11. Hance, T.; van Baaren, J.; Vernon, P.; Boivin, G. Impact of extreme temperatures on parasitoids in a climate change perspective. *Ann. Rev. Entomol.* **2007**, *52*, 107–126. [\[CrossRef\]](#)
12. Jeffs, C.T.; Lewis, O.T. Effects of climate warming on host-parasitoid interactions. *Ecol. Entomol.* **2013**, *38*, 209–218. [\[CrossRef\]](#)
13. Godfray, H.C.J. *Parasitoids: Behavioral and Evolutionary Ecology*; Princeton University Press: Princeton, NJ, USA, 1994.
14. Voigt, W.; Perner, J.; Davis, A.J.; Eggers, T.; Schumacher, J.; Bährmann, R.; Fabian, B.; Heinrich, W.; Köhler, G.; Lichter, D.; et al. Trophic levels are differentially sensitive to climate. *Ecology* **2003**, *84*, 2444–2453. [\[CrossRef\]](#)
15. Harvey, J.A. Conserving host–parasitoid interactions in a warming world. *Curr. Opin. Insect Sci.* **2015**, *12*, 79–85. [\[CrossRef\]](#)
16. Stireman, J.O.; Dyer, L.A.; Janzen, D.H.; Singer, M.S.; Lill, J.T.; Marquis, R.J.; Ricklefs, R.E.; Gentry, G.L.; Hallwachs, W.; Coley, P.D.; et al. Climatic unpredictability and parasitism of caterpillars: Implications of global warming. *Proc. Natl. Acad. Sci. USA* **2005**, *102*, 17384–17387. [\[CrossRef\]](#) [\[PubMed\]](#)
17. Tougeron, K.; Le Lann, C.; Brodeur, J.; Van Baaren, J. Are aphid parasitoids from mild winter climates losing their winter diapause? *Oecologia* **2017**, *183*, 619–629. [\[CrossRef\]](#)
18. Senior, V.L.; Evans, L.C.; Leather, S.R.; Oliver, T.H.; Evans, K.L. Phenological responses in a sycamore–aphid–parasitoid system and consequences for aphid population dynamics: A 20 year case study. *Glob. Chang. Biol.* **2020**, *26*, 2814–2828. [\[CrossRef\]](#)
19. Van Nouhuys, S.; Lei, G. Parasitoid–host metapopulation dynamics: The causes and consequences of phenological asynchrony. *J. Anim. Ecol.* **2004**, *73*, 526–535. [\[CrossRef\]](#)
20. Nealis, V.G. Comparative ecology of conifer-feeding spruce budworms (Lepidoptera: Tortricidae). *Can. Entomol.* **2016**, *148* (Suppl. 1), S33–S57. [\[CrossRef\]](#)
21. Royama, T.; Eveleigh, E.S.; Morin, J.R.B.; Pollock, S.J.; McCarthy, P.C.; McDougall, G.A.; Lucarotti, C.J. Mechanisms underlying spruce budworm outbreak processes as elucidated by a 14-year study in New Brunswick, Canada. *Ecol. Monogr.* **2017**, *87*, 600–631. [\[CrossRef\]](#)
22. Bouchard, M.; Martel, V.; Régnière, J.; Therrien, P.; Correia, D.L.P. Do natural enemies explain fluctuations in low-density spruce budworm populations? *Ecology* **2018**, *99*, 2047–2057. [\[CrossRef\]](#)
23. Régnière, J.; Cooke, B.; Béchard, A.; Dupont, A.; Therrien, P. Dynamics and management of rising outbreak spruce budworm populations. *Forests* **2019**, *10*, 748. [\[CrossRef\]](#)
24. Cusson, M.; Barron, J.R.; Goulet, H.; Régnière, J.; Doucet, D. Biology and status of *Tranosema rostrale rostrale* (Hymenoptera: Ichneumonidae), a parasitoid of the eastern spruce budworm (Lepidoptera: Tortricidae). *Ann. Entomol. Soc. Am.* **1998**, *91*, 87–93. [\[CrossRef\]](#)
25. Fidgen, J.G.; Eveleigh, E.S. Life history characteristics of *Elachertus cacoeciae* (Hymenoptera: Eulophidae), an ectoparasitoid of spruce budworm larvae, *Choristoneura fumiferana* (Lepidoptera: Tortricidae). *Can. Entomol.* **1998**, *130*, 215–229. [\[CrossRef\]](#)
26. Shaw, M.R. Anatomy, reach and classification of the parasitoid complex of a common British moth, *Anthophila fabriciana* (L.) (Choreutidae). *J. Nat. Hist.* **2017**, *51*, 1119–1149. [\[CrossRef\]](#)
27. Seehausen, M.L. Life-History traits and temperature-dependent performance of *Tranosema rostrale* (Hym.: Ichneumonidae), a parasitoid of low-density spruce budworm (Lepidoptera: Tortricidae) populations. Ph.D. Thesis, University of Toronto, Toronto, ON, Canada, 2017.
28. Eveleigh, E.S.; Royama, T.; Lucarotti, C.J.; McCarthy, P.C.; Morin, B.; Pollock, S. Endemic spruce budworm populations in New Brunswick. In Proceedings of the 17th Eastern Spruce Budworm Research Work Conference, Quebec, QC, Canada, 2–3 April 1997; Delisle, J., Régnière, J., Eds.; Info. Rep. LAU-X-113B. Canadian Forest Service, Laurentian Forestry Centre: Quebec, QC, Canada, 1997.
29. Miller, C.A. Parasites and the spruce budworm. *Mem. Entomol. Soc. Can.* **1963**, *95*, 228–244. [\[CrossRef\]](#)
30. Miller, C.A.; Renault, T.R. Incidence of parasitoids attacking endemic spruce budworm (Lepidoptera: Tortricidae) populations in New Brunswick. *Can. Entomol.* **1976**, *108*, 1045–1052. [\[CrossRef\]](#)

31. Seehausen, M.L.; Labrecque, M.; Martel, V.; Régnière, J.; Mansour, A.; Smith, S.M. Reproductive biology and behavior of *Tranosema rostrale* (Hymenoptera: Ichneumonidae), a parasitoid of low-density spruce budworm (Lepidoptera: Tortricidae) populations. *J. Insect Behav.* **2016**, *29*, 500–514. [\[CrossRef\]](#)
32. Seehausen, M.L.; Régnière, J.; Martel, V.; Smith, S.M. Seasonal parasitism and host instar preference by the spruce budworm (Lepidoptera: Tortricidae) larval parasitoid *Tranosema rostrale* (Hymenoptera: Ichneumonidae). *Environ. Entomol.* **2016**, *45*, 1123–1130. [\[CrossRef\]](#)
33. Shaw, M.R.; Horstmann, K.; Whiffin, A.L. Two hundred and twenty-five species of reared western Palaearctic Campopleginae (Hymenoptera: Ichneumonidae) in the National Museums of Scotland, with descriptions of new species of *Campoplex* and *Diadegma*, and records of fifty-five species new to Britain. *Entomol. Gaz.* **2016**, *66*, 245–247.
34. Gangavalli, R.R.; Aliniaze, T. Diapause induction in the oblique-banded leafroller *Choristoneura rosaceana* (Lepidoptera: Tortricidae): Role of photoperiod and temperature. *J. Insect Phys.* **1985**, *31*, 831–835. [\[CrossRef\]](#)
35. Seehausen, M.L.; Régnière, J.; Martel, V.; Smith, S.M. Developmental and reproductive responses of the spruce budworm (Lepidoptera: Tortricidae) parasitoid *Tranosema rostrale* (Hymenoptera: Ichneumonidae) to temperature. *J. Insect Physiol.* **2017**, *98*, 38–46. [\[CrossRef\]](#) [\[PubMed\]](#)
36. Gangavalli, R.R.; Aliniaze, T. Temperature requirements for development of the obliquebanded leafroller, *Choristoneura rosaceana* (Lepidoptera: Tortricidae). *Environ. Entomol.* **1985**, *14*, 17–19. [\[CrossRef\]](#)
37. Jones, V.P.; Doerr, M.D.; Brunner, J.F.; Baker, C.C.; Wilburn, T.D.; Wiman, N.G. A synthesis of the temperature-dependent development rate of the obliquebanded leafroller, *Choristoneura rosaceana*. *J. Insect Sci.* **2005**, *5*, 24. [\[CrossRef\]](#) [\[PubMed\]](#)
38. Aliniaze, M.T. Seasonal history, adult flight activity, and damage of the obliquebanded leafroller, *Choristoneura rosaceana* (Lepidoptera: Tortricidae), in filbert orchards. *Can. Entomol.* **1986**, *118*, 353–361. [\[CrossRef\]](#)
39. Lethiecq, J.L.; Régnière, J. *CFS Spruce Budworm Population Studies: Sites Descriptions*; Info. Rep. LAU-X-83; Canadian Forest Service, Laurentian Forestry Centre: Quebec, QC, Canada, 1988.
40. Seehausen, M.L.; Régnière, J.; Bause, E. Does spruce budworm (Lepidoptera: Tortricidae) rearing diet influence larval parasitism? *Can. Entomol.* **2013**, *345*, 539–542. [\[CrossRef\]](#)
41. Roe, A.R.; Demidovich, M.; Dedes, J. Origins and history of laboratory insect stocks in a multispecies insect production facility, with the proposal of standardized nomenclature and designation of formal standard names. *J. Insect Sci.* **2018**, *18*, 1–9. [\[CrossRef\]](#)
42. Holling, C.S. The functional response of invertebrate predators to prey density. *Mem. Entomol. Soc. Can.* **1966**, *48*, 1–88. [\[CrossRef\]](#)
43. Miller, C.A. The measurement of spruce budworm populations and mortality during the first and second larval instars. *Can. J. Zool.* **1958**, *36*, 409–422. [\[CrossRef\]](#)
44. Tougeron, K.; Brodeur, J.; Le Lann, C.; van Baaren, J. How climate change affects the seasonal ecology of insect parasitoids. *Ecol. Entomol.* **2020**, *45*, 167–181. [\[CrossRef\]](#)
45. Régnière, J.; Powell, J.A. Animal life cycle models (poikilotherms). In *Phenology: An Integrative Environmental Science*, 2nd ed.; Schwartz, M., Ed.; Springer: New York, NY, USA, 2013; pp. 295–316. [\[CrossRef\]](#)
46. Régnière, J.; St-Amant, R.; Béchard, A. *BioSIM 10—User's Manual*; Info. Rep. LAU-X-155; Canadian Forest Service, Laurentian Forestry Centre: Quebec, QC, Canada, 2014.
47. Régnière, J.; Bolstad, P. Statistical simulation of daily air temperature patterns in eastern North America to forecast seasonal events in insect pest management. *Environ. Entomol.* **1994**, *23*, 1368–1380. [\[CrossRef\]](#)
48. Régnière, J. Generalized approach to landscape-wide seasonal forecasting with temperature-driven simulation models. *Environ. Entomol.* **1996**, *25*, 869–881. [\[CrossRef\]](#)
49. Brown, R.D.; Brasnett, B.; Robinson, D. Gridded North American snow depth and snow water equivalent for GCM evaluation. *Atmos. Ocean* **2003**, *41*, 1–14. [\[CrossRef\]](#)
50. Régnière, J.; St-Amant, R. Stochastic simulation of daily air temperature and precipitation from monthly normals in North America north of Mexico. *Int. J. Biometeorol.* **2007**, *51*, 415–430. [\[CrossRef\]](#) [\[PubMed\]](#)
51. Scinocca, J.F.; Kharin, V.V.; Jiao, Y.; Qian, M.W.; Lazare, M.; Solheim, L.; Flato, G.M. Coordinated global and regional climate modeling. *J. Clim.* **2016**, *29*, 17–35. [\[CrossRef\]](#)
52. Arora, V.K.; Scinocca, J.F.; Boer, G.J.; Christian, J.R.; Denman, K.L.; Flato, G.M.; Kharin, V.V.; Lee, W.G.; Merryfield, W.J. Carbon emission limits required to satisfy future representative concentration pathways of greenhouse gases. *Geophys. Res. Lett.* **2011**, *38*, L05805. [\[CrossRef\]](#)

53. Pachauri, R.K.; Allen, M.R.; Barros, V.R.; Broome, J.; Cramer, W.; Christ, R.; Church, J.A.; Clarke, L.; Dahe, Q.; Dasgupta, P.; et al. *Climate Change 2014: Synthesis Report. Contribution of Working Groups I, II and III to the Fifth Assessment Report of the Intergovernmental Panel on Climate Change*; Pachauri, R.K., Meyer, L.A., Eds.; International Panel on Climate Change: Geneva, Switzerland, 2014; p. 151. Available online: <https://www.ipcc.ch/report/ar5/syr> (accessed on 3 August 2020).
54. Canadian Centre for Climate Modelling and Analysis (CCCma) Climate Model Data, CanESM2/CGCM4 Model Output, 2018. Available online: <http://climate-modelling.canada.ca/climatemodeldata/cgcm4/CanESM2/rcp45/> (accessed on 3 August 2020).
55. Liebhold, A.M.; Rossi, R.E.; Kemp, W.P. Geostatistics and geographic information systems in applied insect ecology. *Ann. Rev. Entomol.* **1993**, *38*, 303–327. [[CrossRef](#)]
56. Cusson, M.; Laforge, L.; Régnière, J.; Béliveau, C.; Trudel, D.; Thireau, J.-C.; Bellemare, G.; Keirstead, N.; Stoltz, D. Multiparasitism of *Choristoneura fumiferana* by the ichneumonid *Tranosema rostrale* and the tachinid *Actia interrupta*: Occurrence in the field and outcome of competition under laboratory conditions. *Entomol. Exp. Appl.* **2002**, *102*, 125–133. [[CrossRef](#)]
57. Weisser, W.W.; Volkl, W.; Hassell, M.P. The importance of adverse weather conditions for behaviour and population ecology of an aphid parasitoid. *J. Anim. Ecol.* **1997**, *66*, 386–400. [[CrossRef](#)]
58. Seehausen, M.L.; Cusson, M.; Régnière, J.; Bory, M.; Stewart, D.; Djoumad, A.; Smith, S.M.; Martel, V. High temperature induces downregulation of polydnavirus gene transcription in lepidopteran host and enhances accumulation of host immunity transcripts. *J. Insect Physiol.* **2017**, *98*, 126–133. [[CrossRef](#)]
59. Seehausen, M.L.; Naumann, P.H.; Béliveau, C.; Martel, V.; Cusson, M. Impact of rearing temperature on encapsulation and the accumulation of transcripts putatively involved in capsule formation in a parasitized lepidopteran host. *J. Insect Physiol.* **2018**, *107*, 244–249. [[CrossRef](#)]
60. Bouchard, M.; Auger, I. Influence of environmental factors and spatio-temporal covariates during the initial development of a spruce budworm outbreak. *Landsc. Ecol.* **2014**, *29*, 111–126. [[CrossRef](#)]
61. Bouchard, M.; Régnière, J.; Therrien, P. Bottom-up factors contribute to large-scale synchrony in spruce budworm populations. *Can. J. For. Res.* **2017**, *48*, 277–284. [[CrossRef](#)]
62. Régnière, J.; Nealis, V.G. Density dependence of egg recruitment and moth dispersal in spruce budworms. *Forests* **2019**, *10*, 706. [[CrossRef](#)]
63. Williams, D.W.; Liebhold, A.M. Latitudinal shifts in spruce budworm (Lepidoptera: Tortricidae) outbreaks and spruce-fir forest distributions with climate change. *Acta Phytopathol. Entomol. Hung.* **1997**, *32*, 205–215.
64. Candau, J.-N.; Fleming, R.A. Forecasting the response of spruce budworm defoliation to climate change in Ontario. *Can. J. For. Res.* **2011**, *41*, 1948–1960. [[CrossRef](#)]
65. Gray, D.R. The influence of forest composition and climate on outbreak characteristics of the spruce budworm in eastern Canada. *Can. J. For. Res.* **2013**, *43*, 1181–1195. [[CrossRef](#)]
66. Fleming, R.A.; Volney, W.J.A. Effects of climate change on insect defoliator population processes in Canada's boreal forest: Some plausible scenarios. *Water Air Soil Pollut.* **1995**, *82*, 445–454. [[CrossRef](#)]
67. Régnière, J.; Powell, J.; Bentz, B.; Nealis, V.G. Effects of temperature on development, survival and reproduction of insects: Experimental design, data analysis and modeling. *J. Insect Physiol.* **2012**, *58*, 634–647. [[CrossRef](#)]
68. Fleming, R.A. A mechanistic perspective of possible influences of climate change on defoliating insects in North America's boreal forests. *Silva Fenn.* **1996**, *30*, 281–294. [[CrossRef](#)]
69. Klapwijk, M.J.; Gröbler, B.C.; Ward, K.; Wheeler, D.; Lewis, O.T. Influence of experimental warming and shading on host–parasitoid synchrony. *Glob. Chang. Biol.* **2010**, *16*, 102–112. [[CrossRef](#)]
70. Johnston, A.S.A.; Boyd, R.J.; Watson, J.W.; Paul, A.; Evans, L.C.; Gardner, E.L.; Boulton, V.L. Predicting population responses to environmental change from individual-level mechanisms: Towards a standardized mechanistic approach. *R. Soc. Proc. B* **2019**, *286*, 20191916. [[CrossRef](#)]
71. Maltais, J.; Régnière, J.; Cloutier, C.; Hébert, C.; Perry, D.F. Seasonal biology of *Meteorus trachynotus* Vier. (Hymenoptera: Braconidae) and of its overwintering host *Choristoneura rosaceana* (Harr.) (Lepidoptera: Tortricidae). *Can. Entomol.* **1989**, *121*, 745–756. [[CrossRef](#)]
72. Johns, C.R.; Bowden, J.B.; Carleton, R.D.; Cooke, B.J.; Edwards, S.; Emilson, E.J.S.; James, P.M.A.; Kneeshaw, D.; MacLean, D.A.; Martel, V.; et al. A conceptual framework for the spruce budworm early intervention strategy: Can outbreaks be stopped? *Forests* **2019**, *10*, 910. [[CrossRef](#)]

73. Schmitz, O.J.; Barton, B.T. Climate change effects on behavioral and physiological ecology of predator-prey interactions: Implications for conservation biological control. *Biol. Control* **2014**, *75*, 87–96. [[CrossRef](#)]
74. Gherman, A.-L.M.; Hall, R.J.; Byers, J.E. Host and parasite thermal ecology jointly determine the effect of climate warming on epidemic dynamics. *Proc. Natl. Acad. Sci. USA* **2018**, *115*, 744–749. [[CrossRef](#)]
75. Durant, J.M.; Molinera, J.-C.; Ottersen, G.; Reygondeau, G.; Stige, L.C.; Langangen, O. Contrasting effects of rising temperatures on trophic interactions in marine ecosystems. *Sci. Rep.* **2019**, *9*, 15213. [[CrossRef](#)]
76. Daugaard, U.; Petchey, O.L.; Pennekamp, F. Warming can destabilize predator-prey interactions by shifting the functional response from Type III to Type II. *J. Anim. Ecol.* **2019**, *88*, 1575–1586. [[CrossRef](#)]



© 2020 by the authors. Licensee MDPI, Basel, Switzerland. This article is an open access article distributed under the terms and conditions of the Creative Commons Attribution (CC BY) license (<http://creativecommons.org/licenses/by/4.0/>).